

## Enhanced Li<sup>+</sup> Binding Energies in Alkylbenzene Derivatives: The Scorpion Effect

Otilia M<sup>ó</sup>,<sup>[b]</sup> Manuel Yáñez,<sup>[b]</sup> Jean-François Gal,<sup>\*,[a]</sup> Pierre-Charles Maria,<sup>[a]</sup> and Michèle Decouzon<sup>[a]</sup>

**Abstract:** The gas-phase lithium cation basicities (LCBs; Gibbs free energy of binding) of ethyl-, *n*-butyl-, and *n*-heptylbenzene have been measured by Fourier transform ion cyclotron resonance (FT-ICR) mass spectrometry. The structures of the corresponding complexes and their relative stabilities were investigated through the use of B3LYP/6-311G<sup>+</sup>(3df,2p)//B3LYP/6-31G(d) density functional theory calculations. For *n*-butylbenzene and *n*-heptylbenzene, the most stable adducts correspond to  $\pi$  complexes in which the alkyl chain coils toward the aromatic ring to favor its interaction with the metal cation. The

extra stabilization provided by the flexible alkyl chain polarized by the charge on Li<sup>+</sup> is named the “scorpion effect”. Conversely, these coiled conformations are among the least stable in the neutral system; they are not all stationary points on the potential-energy surface. The formation of complexes with a coiled alkyl chain leads to a significant enhancement of the Li<sup>+</sup> bonding energies

(LBEs), which are approximately 20–30 kJ mol<sup>-1</sup> higher than those calculated for alkylbenzene  $\pi$  complexes in which an uncoiled chain remains distant from the cation and thus minimizes the scorpion effect. This enhancement is less significant when LCBs are concerned, because the scorpion effect is entropically disfavored. There is very good agreement between the experimental Li<sup>+</sup> gas-phase basicities and the calculated values, provided that the statistical distribution of the conformers present in the gas phase is taken into account in this calculation.

**Keywords:** lithium cation affinity • density functional calculations • noncovalent interactions • pi interactions • scorpion effect

### Introduction

Cation– $\pi$  interactions are among the important noncovalent ones in the condensed phase, along with more conventional ones such as hydrogen bonding, ion pairing, and hydrophobic interactions.<sup>[1–8]</sup> They are crucial to the understanding of molecular recognition phenomena, and in particular they are involved in protein side-chain interactions, ligand–receptor bonding, ion channels, and biological catalysis, inter alia. Interactions between ions and unsaturated hydrocarbons were characterized in pioneering gas-phase studies by the Beauchamp<sup>[9–11]</sup> and Kebarle<sup>[12]</sup> groups. Studies on the gas-phase interaction between cations and Lewis bases have been largely devoted to alkali metal cations.<sup>[1, 13–17]</sup> Apeloig et al.<sup>[18]</sup>

pointed out that such interactions are predominantly electrostatic; this was later confirmed by other authors.<sup>[19–24]</sup> Quantum chemical calculations are increasingly associated with experimental studies of ion–molecule interactions in the gas phase, with the aim of characterizing the structure of the adducts or products and analyzing the experimental thermochemical data. This was especially useful for establishing the lithium and sodium cation affinity scales.<sup>[14–16, 25]</sup> The most recent quantitative thermochemical data on aromatic compounds<sup>[15, 26–28]</sup> indicate that their bonding to Li<sup>+</sup> and Na<sup>+</sup> is quite strong, and comparable with that of nitrogen- or oxygen-containing bases.

Another interesting peculiarity of alkali metal cations is their ability to yield chelated complexes in which the metal bridges two or more basic centers of the base. Indeed, these bridged structures explained the enhanced Li<sup>+</sup> and Na<sup>+</sup> binding energies of a series of triazoles, tetrazoles,<sup>[20]</sup> and diazines.<sup>[21]</sup> Alcamí et al.<sup>[21]</sup> showed that these bridged structures are stabilized not only by the electrostatic interaction of the metal cation with the basic sites, but also by the polarization of both centers when the metal is more or less equidistant from them.

There were also early indications that a flexible alkyl side chain may interact with a metal cation bonded to a hetero-

[a] Prof. J.-F. Gal, Prof. P.-C. Maria, Dr. Ing. M. Decouzon  
Chimie des Matériaux Organiques et Métalliques  
Université de Nice-Sophia Antipolis  
Parc Valrose, 06108 Nice Cedex 2 (France)  
Fax: (+33)492-07-61-11  
E-mail: gal@unice.fr

[b] Prof. O. M<sup>ó</sup>, Prof. M. Yáñez  
Departamento de Química, C-9  
Universidad Autónoma de Madrid  
Cantoblanco, 28049-Madrid (Spain)

atom. Allison and co-workers<sup>[29–33]</sup> and Schwarz and co-workers<sup>[34–38]</sup> showed that the alkyl chain might adopt a coiled conformation, favorable to a stabilizing polarization by the charge on the metal ion. In the case of transition-metal ions, such adducts are invoked as a step toward the appearance of a new, distant function. This process was referred to as “remote functionalization”.<sup>[35, 38]</sup> By contrast, alkali metal ions form stable adducts (with a few exceptions<sup>[9, 30]</sup>) with a variety of organic molecules. Along with the ease of producing alkali metal ions in the gas phase, this allowed the building of comprehensive affinity scales. The Li<sup>+</sup> basicity scale was developed extensively by Taft and collaborators.<sup>[1, 14]</sup> In particular the effect of alkyl groups on the lithium cation basicity of several series of bases was assessed. It was suggested that “alkyl groups can enter into chelate formation with Li<sup>+</sup> by closing a five- or larger-membered ring through a charge induced dipole interaction of sufficient magnitude to overcome the entropy loss of ring formation”.<sup>[1]</sup> This hypothesis has been substantiated by *ab initio* calculations on alcohols.<sup>[39, 40]</sup>

The aim of this paper is to show that cation/ $\pi$  complexes can also clearly be stabilized in the gas phase by alkyl chains of sufficient length, with three or more carbon atoms, as substituents in aromatic systems. Compounds with high dipole moments have the highest affinities for alkali metal ions, but saturated and unsaturated hydrocarbons also exhibit significant binding energies for these ions. We explore, both experimentally and theoretically, cooperative effects of typically nonpolar moieties, such as the benzene ring and alkyl chains of varying length, on Li<sup>+</sup> bonding.

For this purpose, the gas-phase lithium cation basicity (LCB, also designated  $\Delta G(\text{Li}^+)$ ), defined as the Gibbs free energy of a base B for the process represented by Equation (1), was measured by Fourier transform ion cyclotron resonance (FT-ICR) mass spectrometry for ethyl-, *n*-butyl-, and *n*-heptylbenzene, and compared with the values estimated by high-level density functional theory calculations.



**FT-ICR measurements:** Lithium-cation-transfer equilibrium constants were determined by a method similar to that described by Burk et al.<sup>[14]</sup> The main differences were the Li<sup>+</sup> source and the working temperature. The lithium cation was generated by laser ablation (pulsed nitrogen laser, 337 nm, 200  $\mu\text{J}$  per pulse) from a lithium benzoate target, as a pellet obtained by compression of the salt.<sup>[41]</sup> A small amount of 2-chloropropane was added to the system under scrutiny to generate the propene/Li<sup>+</sup> adduct, which in turn transferred Li<sup>+</sup> to ligands of larger LCB. Equilibrium constants were determined at three or more different pressure ratios. The total pressure, in the 10<sup>−5</sup> Pa range, was measured with an ion gauge. Reaction times were about 10 s. As there was no heat source close to the ICR cell (except for the electromagnet poles at about 30 °C, which were outside the vacuum chamber), the experiments were conducted at close to 25 °C (298 K). The experimental determination of the LCB for ethyl-, *n*-butyl-, and *n*-heptylbenzene relied on 12 equilibrium measurements;  $\Delta\text{LCB}$  is reported in Table 1.

Table 1. Lithium cation basicity (LCB [kJ mol<sup>−1</sup>] at 373 K<sup>[a]</sup>) for ethylbenzene, *n*-butylbenzene, and *n*-heptylbenzene.

Compound (B)	Reference (B <sub>ref</sub> )	$\Delta\text{LCB}$ [kJ mol <sup>−1</sup> ]	LCB [kJ mol <sup>−1</sup> ]	
			B <sub>ref</sub> <sup>[b]</sup>	B <sup>[b]</sup>
Ph–Et	CF <sub>3</sub> CH <sub>2</sub> OH		110.9 <sup>[c]</sup>	
	Ph–CH=CH <sub>2</sub>	+ 7.20(±0.50)	122.7	130.2
	Ph–Me	+ 5.90 ± 0.46	124.2	
	MeCHO	− 0.63 ± 0.89	130.4	
Ph– <i>n</i> Bu	EtCHO	− 6.53 ± 0.20	136.3	
	P–Et	+ 8.00 ± 0.15	130.2	136.4
	EtCHO	− 0.24 ± 0.22	136.3	
	<i>n</i> PrCHO	− 2.90 ± 0.17	139.0	
	Et <sub>2</sub> O	− 3.48 ± 0.13	140.4	
Ph–(CH <sub>2</sub> ) <sub>6</sub> –Me	Et <sub>2</sub> O	+ 10.06 ± 0.14	140.4	150.1
	( <i>n</i> Pr) <sub>2</sub> O	− 0.22 ± 0.10	150.0	
	Me <sub>2</sub> CO	− 1.13 ± 0.11	151.1	
	( <i>i</i> Pr) <sub>2</sub> O	− 1.38 ± 0.31	151.5	

[a] Temperature of the reference scale;<sup>[14]</sup> see text. [b] LCBs for the compounds (B) studied here and for the compounds used as references (B<sub>ref</sub>) obtained by a Free–Wilson treatment; see text. [c] All values are anchored to the experimental LCB of CF<sub>3</sub>CH<sub>2</sub>OH,<sup>[14, 26]</sup> which is the least basic compound of the series involved in the Free–Wilson treatment.

Relative LCBs of the three compounds were inferred from a simultaneous optimization of the overlap of these experimental data, together with 47 previously determined  $\Delta\text{LCBs}$  involving 29 compounds ranging (in order of increasing LCB) from 2,2,2-trifluoroethanol to diisopropyl ether (16 reference compounds;<sup>[14]</sup> six benzene derivatives;<sup>[26]</sup> the three alkylbenzenes studied here; naphthalene, phenanthrene, anthracene, and azulene<sup>[56]</sup>). The 59  $\Delta\text{LCBs}$  considered were treated by a multiple linear regression procedure as used by Taft and co-workers<sup>[42]</sup> and according to the Free and Wilson treatment.<sup>[43]</sup> Each experimental  $\Delta\text{LCB}$  was described by a series of 1 (presence) or 0 (absence) of LCB intervals with no constant term being included in the model. This led to a model explaining 99.05% of the variance in the experiments.

Theoretical estimates showed that the change in LCB between 298 K and 373 K is nearly constant (5.5–6.7 kJ mol<sup>−1</sup>) for different compounds. Therefore the errors introduced by combining relative room-temperature LCB values with the 373 K scale without temperature correction were expected to be less than 1.2 kJ mol<sup>−1</sup> in general. In this work, the values are anchored arbitrarily to the compound of weakest basicity, CF<sub>3</sub>CH<sub>2</sub>OH. The resulting absolute LCB values in Table 1 agree to within  $\pm 3$  kJ mol<sup>−1</sup> with the values published in our previous study,<sup>[14]</sup> but the *relative* values are more accurate, with uncertainties of the order of 1 kJ mol<sup>−1</sup> or less. Comparison of the values obtained for substituted benzenes and auxiliary compounds used to link them (Table 1) with other published scales demonstrates that uncertainties in *absolute* LCB values are greater in general, in the  $\pm 5$ –15 kJ mol<sup>−1</sup> range.

## Computational Methods

The B3LYP density functional theory method, as implemented in the Gaussian-98 series of programs,<sup>[44]</sup> which combines Becke's three-parameter nonlocal hybrid exchange potential<sup>[45, 46]</sup> with the nonlocal correlation

functional of Lee et al.,<sup>[47]</sup> is very well suited for the description of metal ion complexes and for obtaining metal cation binding energies in fairly good agreement with the experimental values.<sup>[48, 49]</sup> Its performance when applied to  $\text{Li}^+$  complexes has been assessed in several combined theoretical and experimental studies.<sup>[14, 26, 48]</sup> Hence, we adopted this theoretical method. The geometries of the alkylbenzene derivatives and their  $\text{Li}^+$  complexes were optimized by using a 6-31G(d) basis set expansion. The same basis set was used to calculate the harmonic vibrational frequencies, which allowed us to characterize the different stationary points as true local minima of the potential-energy surface (PES) and to estimate the zero-point energy (ZPE) corrections, as well as the vibrational thermal corrections. The translational, rotational, and  $PV$  thermal contributions were estimated as  $(\frac{3}{2})RT$ ,  $(\frac{3}{2})RT$ , and  $RT$ , respectively. The corresponding LBEs were evaluated by subtracting the energies of neutral species and of  $\text{Li}^+$  from the energy of the complex, after including the ZPE corrections and the aforementioned thermal corrections at 373 K (the temperature of the reference scale used to anchor our data).

Final energies were evaluated in single-point calculations at the B3LYP/6-311G<sup>+</sup>(3df,2p) level. For *n*-heptylbenzene (1-phenylheptane), these calculations were carried out only for the following systems: 1) the neutral conformers whose energies lie less than 7 kJ mol<sup>-1</sup> above the global minimum, and their  $\text{Li}^+$  complexes; 2) the  $\text{Li}^+$  complexes whose energies lie less than 7 kJ mol<sup>-1</sup> above the energy of the most stable one, and the neutral species from which they are obtained.

For *n*-butylbenzene, but especially for *n*-heptylbenzene, it would be an enormous task to account for all the conformers. Nevertheless, to consider the most important ones systematically, we took as a starting point the global minimum of the PES, the **Hept1** conformer, in which the alkyl chain is completely extended. We considered the isomers that could be formed by

torsion around the C1–C2, C2–C3, C3–C4, C4–C5, and C5–C6 bonds (numbering as in Figure 1). The C1–C2 torsion would yield a conformer with the alkyl chain in the same plane as the aromatic ring, but this conformation is not a stationary point of the PES as it collapses to the global minimum. The same behavior was observed for the *n*-propyl and *n*-butyl derivatives. The C2–C3, C3–C4, C4–C5, C5–C6, and C6–C7 torsions yield **Hept2**, **Hept1a**, **Hept1b**, **Hept1c**, and **Hept1d** conformers, respectively (see Figure 1). Each of the conformers generated in this way can now be taken as a precursor of new conformers by successive C–C torsions. For instance, starting from the **Hept2** conformer, C3–C4, C4–C5, C5–C6, and C6–C7 torsions yield **Hept2a**, **Hept2b**, **Hept2c**, and **Hept2d** species, respectively. Many of these possibilities, although not all, have been explored, but for conciseness in the discussion that follows we shall concentrate exclusively on the most stable ones to systematize the discussion; these were numbered in order of stability. The omission of many possible conformers from our survey has no significant effect on our calculated values for the binding energies, as most of them lie more than 7 kJ mol<sup>-1</sup> above the global minimum and, therefore, would not contribute significantly to the macroscopic thermochemistry at the experimental temperature. Some others are very close in energy to, or almost degenerate with, those considered in our calculations, and therefore their inclusion would not change the calculated binding energies significantly.

## Results and Discussion

**Structures and relative stabilities:** Schematized structures of ethyl-, *n*-propyl-, and *n*-butylbenzene and of the  $\text{Li}^+$  com-

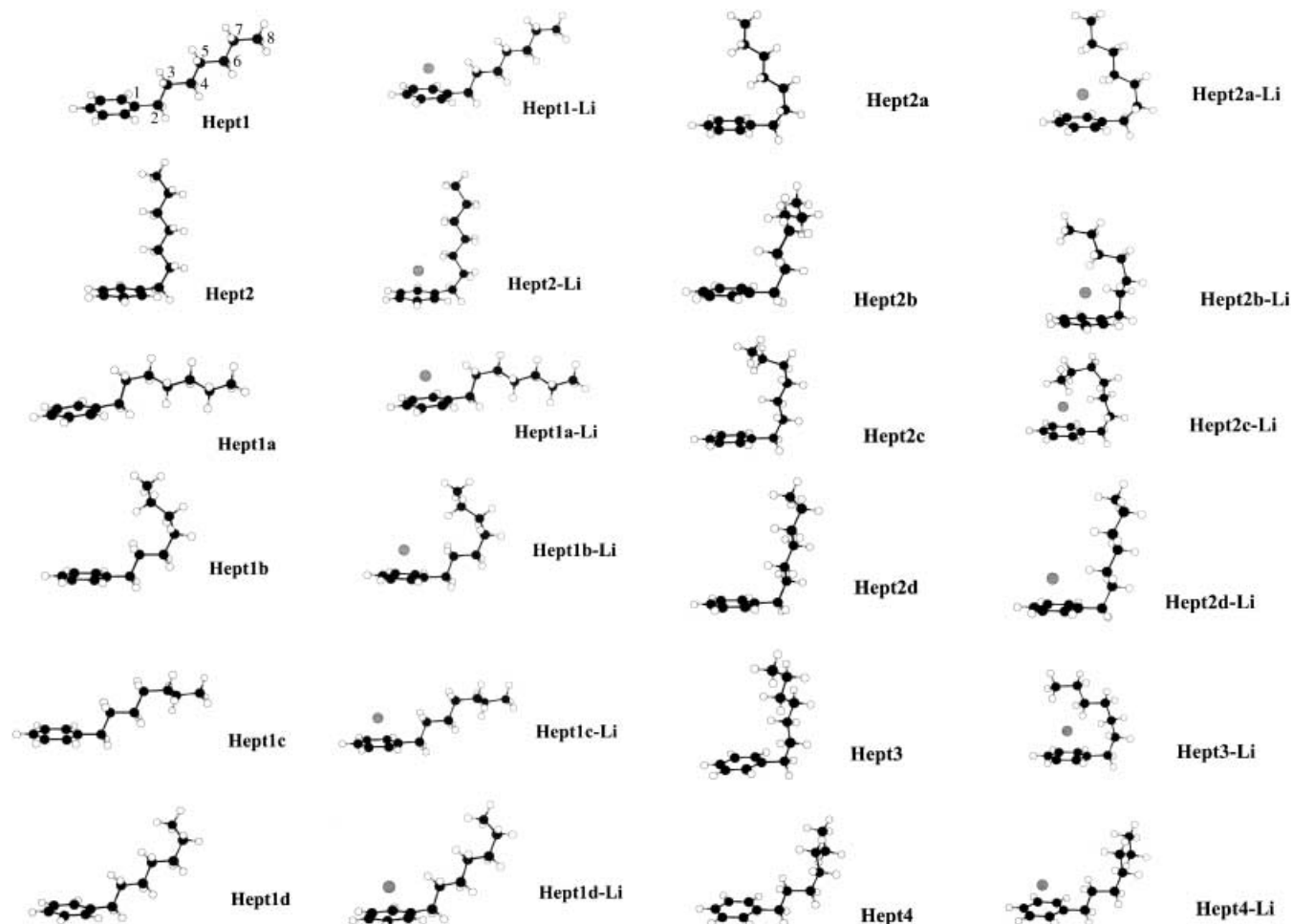


Figure 1. Schematic representation of the B3LYP/6-31G(d)-optimized geometries for the conformers of *n*-heptylbenzene (1-phenylheptane) and their  $\text{Li}^+$  complexes. The carbon numbering used for *n*-heptylbenzene is given (see **Hept1**).

plexes obtained for each conformer are shown in Figure 2. Their total energies, LBEs, and LCBs are summarized in Table 2.

Experimental determination of the LCB of *n*-propylbenzene was not essential for this study, but we included this compound in our theoretical survey to visualize better the

Table 2. DFT-calculated total energy ( $E$  [hartrees]), zero-point energy (ZPE [hartrees]), entropy ( $S$  [J mol<sup>-1</sup>K<sup>-1</sup>]), and relative energy<sup>[a]</sup> for neutral conformers and the corresponding Li<sup>+</sup> complexes ( $\Delta E$  and  $\Delta E_{\text{Li}^+}$ , respectively [kJ mol<sup>-1</sup>]), lithium cation binding energy (LBE [kJ mol<sup>-1</sup>]), lithium cation basicity (LCB [kJ mol<sup>-1</sup>]) for alkylbenzene derivatives (1 hartree = 2625.50 kJ mol<sup>-1</sup>).

System	B3LYP/6-31G*					B3LYP/6-311G <sup>+</sup> (3df,2p)		LCB
	$E$	ZPE	$S$	$\Delta E$	$\Delta E_{\text{Li}^+}$	$E$	LBE	
Li <sup>+</sup>			133.043			-7.284918		
Et	-310.88025	0.15746	354.883			-310.98379		
Et-Li	-318.23716	0.16010	377.648			-318.33605	173	132
<i>n</i> Pro1	-350.19428	0.18600	386.392	0.0		-350.31072		
<i>n</i> Pro1-Li	-357.55244	0.18867	408.596		1.0	-357.66409	176	133
<i>n</i> Pro2	-350.19346	0.18618	383.572	2.6		-350.30963		
<i>n</i> Pro2-Li	-357.55272	0.18858	400.819		0.0	-357.66376	178	177 <sup>[b]</sup> 135
<i>n</i> But1	-389.50795	0.21456	418.467	0.0		-389.63727		
<i>n</i> But1-Li	-396.86682	0.21722	440.010		4.5	-396.99130	177	135
<i>n</i> But2	-389.50717	0.21481	414.316	2.7		-389.63623		
<i>n</i> But2-Li	-396.86775	0.21714	430.178		1.9	-396.99152	182	138
<i>n</i> But3	-389.50355	0.21480	414.496	12.2		-389.63235		
<i>n</i> But3-Li	-396.86932	0.21799	413.931		0.0	-396.99313	195	145
<i>n</i> But4	-389.50659	0.21458	421.931	3.6		-389.63587		
<i>n</i> But4-Li	-396.86558	0.21721	446.190		7.8	-396.99056	182	141
<i>n</i> But5	-389.50581	0.21487	414.329	6.4		-389.63476		
<i>n</i> But5-Li	-396.86630	0.21721	428.927		5.9	-396.99001	182	178 <sup>[b]</sup> 138

[a] Relative energies were obtained at the B3LYP/6-31G\* level and include the corresponding ZPE correction. [b] Values obtained by taking into account the statistical distribution of the most stable conformers of reactants and products; see text.

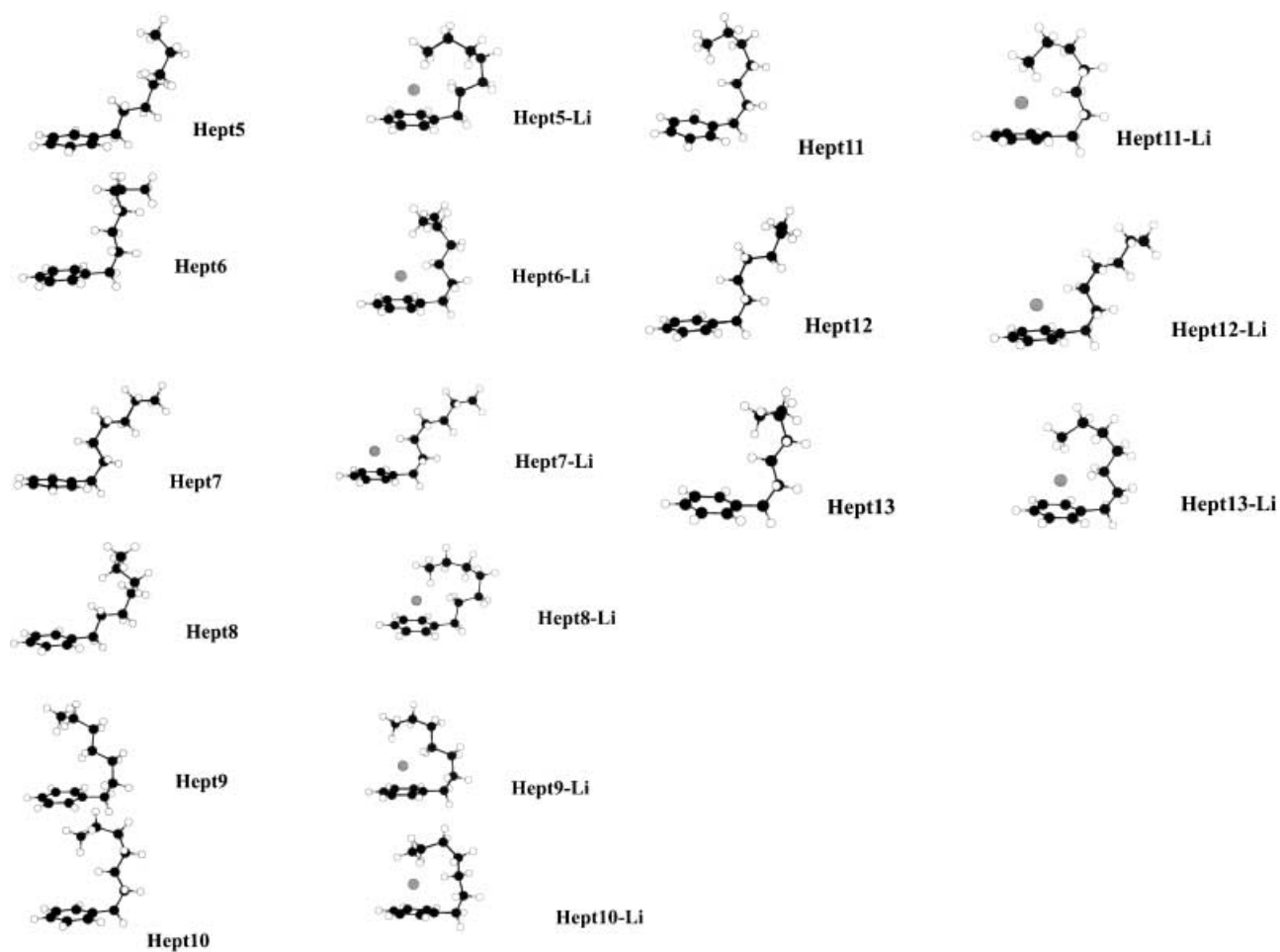


Figure 1. Continued.

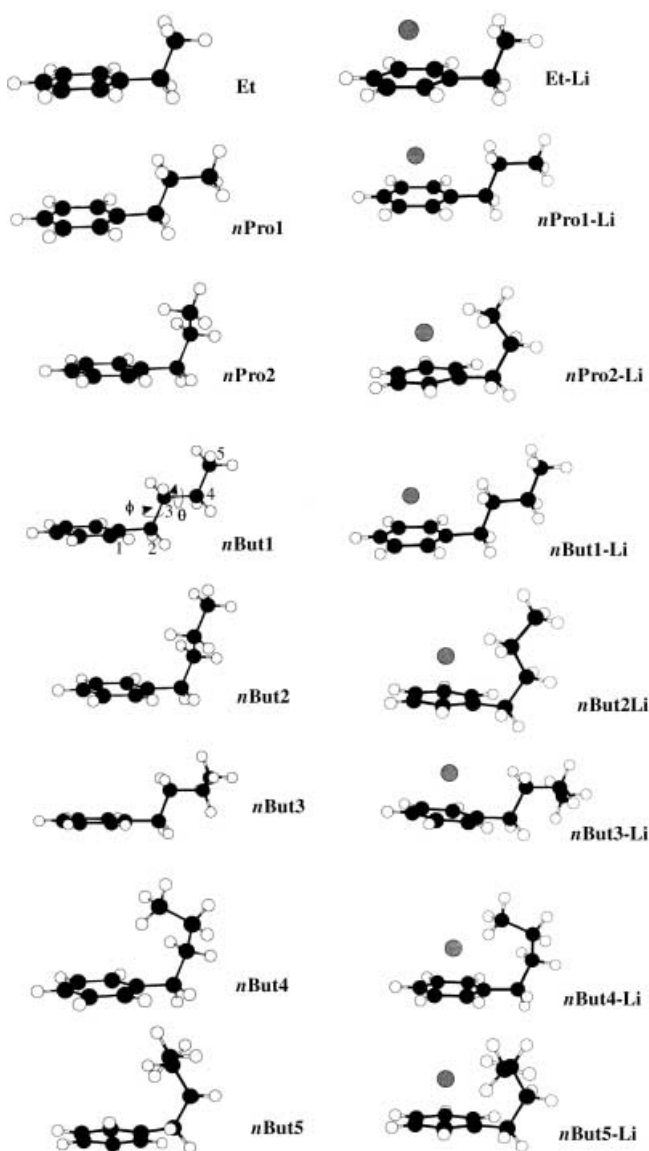


Figure 2. Schematic representation of the B3LYP/6-31G(d)-optimized geometries for the ethyl-, *n*-propyl-, and *n*-butylbenzene conformers and their Li<sup>+</sup> complexes;  $\phi$  and  $\theta$  are the torsional angles connecting the different conformers of *n*-butylbenzene. The carbon numbering used for *n*-butylbenzene is given (see **nBut1**).

evolution of the conformational changes as the alkyl chain length increases. For ethylbenzene, only the conformer in which the carbon of the CH<sub>3</sub> group is in a plane perpendicular to the plane of the aromatic ring is a minimum of the PES. This situation does not change upon Li<sup>+</sup> association. For benzene derivatives like those included in this study, there are always two kinds of  $\pi$  complexes that differ in the relative positions of the metal cation and the alkyl chain: they may be 1) on the same side or 2) on opposite sides of the aromatic ring. We have found systematically that complexes in which the metal and the alkyl chain are on the same side are the most stable. Therefore, we shall hereafter refer exclusively to these complexes.

For *n*-propylbenzene, the two conformers shown in Figure 2 were found to be local minima of the PES, **nPro1** being the more stable. No conformer with the methyl group pointing

toward the aromatic ring was found to be a minimum. Conversely, when the **nPro2** conformer interacts with Li<sup>+</sup>, a spontaneous C1–C2 torsion brings the methyl group closer to the metal cation. Thus, in the **nPro2–Li** complex, Li<sup>+</sup> interacts synergistically with the aromatic  $\pi$  system and with the methyl group of the substituent. This complex is estimated to be 2.5 kJ mol<sup>-1</sup> more stable than **nPro1–Li** (See Table 2).

For *n*-butylbenzene, the **nBut1** conformer (see Figure 2), in which the alkyl chain is completely extended, was estimated to be the global minimum of the PES. The C1–C2 torsion leads to a conformer in which the alkyl chain lies in the plane of the ring. However, as mentioned above, such a conformation is not a stationary point of the PES as it collapses to the global minimum. The C2–C3 torsion leads to the **nBut2** conformer. Once more, the conformer corresponding to a 180° torsion around C2–C3, which brings the terminal CH<sub>2</sub>CH<sub>3</sub> group of the alkyl chain closer to the aromatic ring, is not a local minimum of the PES. However, such a conformation is favored upon interaction with the metal cation, in such a way that in the **nBut2–Li** complex the metal cation interacts simultaneously with the  $\pi$  system and with the  $\gamma$ -methylene group of the butyl substituent. A C3–C4 torsion in **nBut1** would yield the **nBut3** conformer, which is only slightly less stable. A C3–C4 torsion in **nBut2** leads to **nBut4**. Although **nBut4** is the less stable neutral conformer, it yields the most stable Li<sup>+</sup> complex, **nBut4–Li**. Finally, a C2–C3 torsion in **nBut3** yields the **nBut5** conformer.

In summary, the interaction between the alkyl chain and the  $\pi$  system is not favored in the neutral molecule, the global minimum being the conformer in which this chain is completely extended away from the aromatic ring. Conversely, the Li<sup>+</sup> complex in which the chain is completely extended is systematically the less stable one. The stability of the Li<sup>+</sup> complex increases when either a methylene group or the terminal methyl group, or both, approach the metal cation. Consequently the most stable conformation for the **nBut4–Li** complex corresponds systematically to the structure in which the chain is bent toward the metal cation.

For *n*-heptylbenzene, the structures of the most relevant conformers and their Li<sup>+</sup> complexes are given in Figure 1; their energies, the LBEs and the LCBs are collated in Table 3.

As expected, the situation is much more complex than for *n*-propyl- or *n*-butylbenzene because of the huge number of possible conformers. However, the general features observed for the propyl and butyl derivatives hold. The most stable conformers for the neutral species, namely, **Hept1**, **Hept2**, and **Hept1a**, correspond to the situation in which the alkyl chain attains its maximum extension (see Figure 1). Conversely, the most stable complex, **Hept3–Li**, corresponds to a conformation in which the alkyl chain is bent over the metal cation, maximizing the simultaneous interaction of Li<sup>+</sup> with the  $\pi$  system, with two of the methylene groups, and with the terminal methyl group of the substituent. Consistently, the stabilization decreases by 6–14 kJ mol<sup>-1</sup> when one methylene–cation interaction is removed, as is seen for complexes such as **Hept9–Li**, **Hept10–Li**, **Hept11–Li**, and **Hept13–Li**. This stability decreases further when only one methylene group is close to Li<sup>+</sup>, as in **Hept2–Li** or **Hept7–Li** complexes, whereas the least stable complexes, such as **Hept1–Li**,

Table 3. Total energy ( $E$  [hartrees]), zero-point energy (ZPE [hartrees]), entropy ( $S$  [ $\text{J mol}^{-1} \text{K}^{-1}$ ]), relative energy<sup>[a]</sup> for neutral conformers and the corresponding Li<sup>+</sup> complexes ( $\Delta E$  and  $\Delta E_{\text{Li}^+}$ , respectively [ $\text{kJ mol}^{-1}$ ]), Li<sup>+</sup> binding energy (LBE [ $\text{kJ mol}^{-1}$ ]), and lithium cation basicity (LCB [ $\text{kJ mol}^{-1}$ ]) for heptylbenzene.

System	B3LYP/6–31G(d)					B3LYP/6–311 + G(3df,2p)		
	$E$	ZPE	$S$	$\Delta E$	$\Delta E_{\text{Li}^+}$	$E$	LBE	LCB
<b>Hept1</b>	–507.44913	0.30042	514.251	0.0		–507.61709		
<b>Hept1–Li</b>	–514.80869	0.30311	535.029		16.7	–514.97185	179	137
<b>Hept2</b>	–507.44832	0.30063	507.799	2.7		–507.61622		
<b>Hept2–Li</b>	–514.81073	0.30293	527.100		10.9	–514.97387	188	145
<b>Hept1 a</b>	–507.44775	0.30040	514.933	3.6		–507.61564		
<b>Hept1 a–Li</b>	–514.80743	0.30309	535.280		19.9	–514.97056	180	138
<b>Hept1 b</b>	–507.44394	0.30066	511.151	14.2				
<b>Hept1 b–Li</b>	–514.80289	0.30345	530.401		32.8			
<b>Hept1 c</b>	–507.44776	0.30055	511.130	3.9		–507.61565		
<b>Hept1 c–Li</b>	–514.80731	0.30306	542.736		20.2	–514.97039		
<b>Hept1 d</b>	–507.44779	0.30059	511.297	4.0		–507.61570		
<b>Hept1 d–Li</b>	–514.80737	0.30328	533.088		20.6	–514.97049		
<b>Hept2 a</b>	–507.44474	0.30064	507.933	12.1		–507.61225		
<b>Hept2 a–Li</b>	–514.81492	0.30380	506.351		2.1	–514.97642	204	154
<b>Hept2 b</b>	–507.44303	0.30084	505.938	17.1		–507.61062		
<b>Hept2 b–Li</b>	–514.81570	0.30376	505.084		0.0	–514.97737	211	161
<b>Hept2 c</b>	–507.44574	0.30090	510.339	10.2		–507.61334		
<b>Hept2 c–Li</b>	–514.81391	0.30388	499.112		5.0	–514.97474	197	144
<b>Hept2 d</b>	–507.44697	0.30074	507.272	6.5		–507.61460		
<b>Hept2 d–Li</b>	–514.80950	0.30309	527.410		14.5	–514.97162	188	144
<b>Hept3<sup>[b]</sup></b>	–507.44692	0.30080	506.887	12.8		–507.61452		
<b>Hept3–Li</b>	–514.81570	0.30376	505.084		0.0	–514.97737	201	151
<b>Hept4</b>	–507.44649	0.30077	515.113	7.8		–507.61079		
<b>Hept4–Li</b>	–514.80598	0.30330	532.878		24.3	–514.97564	206	152
<b>Hept5</b>	–507.44646	0.30083	508.122	8.1				
<b>Hept5–Li</b>	–514.80400	0.30378	502.582		30.8			
<b>Hept6</b>	–507.44567	0.30095	502.368	10.5				
<b>Hept6–Li</b>	–514.80815	0.30341	517.372		18.9			
<b>Hept7</b>	–507.44689	0.30066	510.017	6.5				
<b>Hept7–Li</b>	–514.80879	0.30312	524.711		16.4			
<b>Hept8</b>	–507.44395	0.30070	511.297	14.3				
<b>Hept8–Li</b>	–514.80228	0.30361	506.243		34.8			
<b>Hept9</b>	–507.44339	0.30073	509.615	15.9		–507.61079		
<b>Hept9–Li</b>	–514.81443	0.30351	504.209		2.7	–514.97561	206	165
<b>Hept10</b>	–507.44308	0.30078	512.519	16.8				
<b>Hept10–Li</b>	–514.81115	0.30358	543.669		11.5			
<b>Hept11</b>	–507.44306	0.30092	506.415	17.2		–507.61066		
<b>Hept11–Li</b>	–514.81364	0.30414	494.975		6.4	–514.97510	205	164
<b>Hept12</b>	–507.44557	0.30092	508.348	10.6				
<b>Hept12–Li</b>	–514.80751	0.30347	518.941		20.7			
<b>Hept13</b>	–507.44298	0.30083	508.260	17.2				
<b>Hept13–Li</b>	–514.81036	0.30392	499.720		14.4		<b>193<sup>[c]</sup></b>	<b>147<sup>[c]</sup></b>

[a] Relative energies were obtained at the B3LYP/6-31G\* level and include the corresponding ZPE correction. [b] Conformer **Hept3** yields the same Li<sup>+</sup> complex as conformer **Hept2b**. [c] Values obtained by taking into account the statistical distribution of the most stable conformers of reactants and products (see text).

**Hept1c–Li**, and **Hept1d–Li**, are those in which the metal cation interacts only with the  $\pi$  system. It is also very important that in many cases the presence of the metal cation triggers the coiling of the alkyl chain. This is clear if one compares the conformation of the **Hept3**, **Hept5**, **Hept6**, **Hept8**, **Hept11**, and **Hept13** species and those of their corresponding Li<sup>+</sup> complexes, for instance. To confirm the presence of this effect, we have also optimized the structures of the neutral systems that result from eliminating the Li<sup>+</sup> cation from each complex. In all cases we arrived, after the geometry optimization, at the aforementioned neutral conformers, so we have confirmed that when the metal cation is not present the alkyl chain relaxes to a less folded conformation, and the **Hept3**, **Hept5**, **Hept6**, **Hept8**, **Hept11**, and **Hept13** conformers are obtained.

Around this general pattern there are some fluctuations due to small differences between the interactions involving the methylene groups of the alkyl chain. This explains, for instance, the stability difference between **Hept2d–Li** and **Hept6–Li**. In both cases the Li<sup>+</sup> cation interacts with the  $\gamma$ -methylene group, but the conformation of the rest of the chain favors a greater stability of the first conformer. In some other cases, slightly different conformers, such as **Hept2b** and **Hept3**, lead to the same complex.

We call the structure of a Li<sup>+</sup> adduct with the alkyl chain bent toward the aromatic ring a “scorpion structure”, by reference to the well-known arachnid in its defense position, with the tail bent over its body. The term “scorpio structure” has been proposed for protonated histamine,<sup>[40, 50, 51]</sup> in which the  $\text{CH}_2\text{CH}_2\text{NH}_2$  side chain is bent toward the protonated

imidazole ring. A “scorpion effect” was also proposed for a transannular interaction favoring a chair conformation in substituted cyclohexane.<sup>[52]</sup>

The scorpion effect is reflected in some peculiarities of the complexes. For complexes in which this effect is not significant, such as **Hept1–Li**, **Hept1a–Li**, **Hept1c–Li**, and **Hept4–Li**, the distance between the metal cation and the plane of the benzene ring is slightly shorter (1.867, 1.843, 1.866, 1.830 Å) than that found, at the same level of accuracy,<sup>[26]</sup> for the benzene–Li<sup>+</sup> complex (1.876 Å). This reflects the intrinsic higher basicity of the heptyl derivative, so the  $\pi$  system of the heptyl derivative becomes a better electron donor because of the effect of the alkyl group. Conversely, in those complexes in which the scorpion effect is important, such as **Hept3–Li**, **Hept5–Li**, and **Hept8–Li**, the distance between the metal cation and the plane of the ring becomes greater (1.914, 1.904, 1.989 Å, respectively), because of the attractive interaction between the metal cation and the alkyl chain.

The formation of complexes such as **Hept1–Li** implies a sizable polarization of the aromatic  $\pi$ -electron density. When the scorpion effect is important, as in **Hept3–Li**, there is also a strong polarization of the charge density of the methyl group and of the methylene groups closest to the metal cation. These polarizations are mirrored in a non-negligible charge transfer from the base toward the Li<sup>+</sup> cation. Hence, while in complexes like **Hept1–Li** the charge transferred is about 0.3 e<sup>-</sup>, in complexes like **Hept3–Li** it is almost 0.5 e<sup>-</sup>. The charge withdrawal from the  $\pi$  cloud results in a slight weakening of all the C–C bonds of the benzene ring, which accordingly lengthen by 0.01 Å on average. For complexes where the scorpion effect appears, there is also a non-negligible lengthening of the C–H bonds of the methylene or methyl groups interacting with the metal cation. The **Hept3–Li** complex is an example: the two C6–H bonds lengthen by 0.10 Å, and the C8–H bond closest to the metal becomes 0.08 Å longer. These changes are also reflected in sizable shifts of the corresponding stretching frequencies (vide infra).

**Vibrational frequencies:** The interaction of Li<sup>+</sup> with the benzene moiety produces a systematic blue shift of all the out-of-plane C–H bending modes, similar to those already reported for other complexes of benzene derivatives with Li<sup>+</sup>.<sup>[26]</sup> All the complexes investigated exhibit a vibration mode in the region 380–400 cm<sup>-1</sup>, which corresponds to the displacement of the metal cation in a direction perpendicular to the aromatic ring ( $\nu_{\text{ring-Li}}$ ), in agreement with previous findings.<sup>[26]</sup>

In complexes in which the scorpion effect is observed, there is also a significant red shift, by as much as 150 cm<sup>-1</sup>, of the C–H stretching frequencies of the CH<sub>2</sub> and CH<sub>3</sub> groups interacting with the metal.

**Lithium cation basicities:** The calculated LBEs and LCBs for ethyl-, *n*-propyl-, and *n*-butylbenzene are summarized in Table 2. For ethylbenzene the agreement between the calculated and experimental values is very good. It is clear from a comparison of the LBEs of **nBut1** and **nBut3** complexes that the scorpion effect accounts for an enhancement of the binding energy of about 18 kJ mol<sup>-1</sup>. This enhancement is

smaller (approximately 10 kJ mol<sup>-1</sup>) for the LCBs, because the scorpion effect is accompanied by a non-negligible decrease in the entropy of the complex (see Table 2). As expected, these effects are quantitatively greater for *n*-heptylbenzene (see Table 3). The difference in the calculated LBEs corresponding to the **Hept1–Li** form (no scorpion effect), and, for instance, the **Hept2b–Li** form (in which this effect operates) is approximately 32 kJ mol<sup>-1</sup>. Again the entropic contribution leads to a smaller difference in LCBs.

However, these values cannot be compared directly with the experimental data. Under normal experimental conditions, the neutral system is a statistical mixture of the most stable conformers. Similarly, the product will also be a statistical mixture of the most stable complexes. Hence, on the basis of the relative Gibbs free energies of the different conformers, *n*-butylbenzene should be an equilibrium mixture of **nBut1** (73%), **nBut4** (18%), and **nBut5** (9%). Similarly, the mixture of Li<sup>+</sup> adducts should be composed of **nBut1–Li** (41%), **nBut4–Li** (32%), **nBut2–Li** (16%), **nBut3–Li** (8%), and **nBut5–Li** (3%). Under this assumption the estimated LCB is 135 kJ mol<sup>-1</sup>, which is in fairly good agreement with the experimental value.

Similarly, *n*-heptylbenzene should be an equilibrium mixture (see Figure 1) of **Hept1** (58%), **Hept1a** (15%), **Hept1c** (10%), **Hept2** (8%), **Hept1b** (7%), and **Hept2d** (2%). The statistical distribution of the products should be **Hept3–Li** (48%), **Hept4–Li** (22%), **Hept2a–Li** (20%), **Hept9–Li** (6%), and **Hept2c–Li** (4%). From these values, the estimated LCB of *n*-heptylbenzene should be 147 kJ mol<sup>-1</sup>, again in good agreement with the experimental value.

It must be taken into account that in this theoretical estimation we have not considered the additional entropy associated with the exploration of several minima of the PES. However, it can reasonably be assumed that these entropy contributions would not be very different for neutral species and Li<sup>+</sup> complexes, and therefore the effect on the calculated LCB must be quite small. Also, as already mentioned, it would be a practically impossible task to consider all possible isomers. This implies that our estimates for the LCBs would be changed if the accessible conformations were substantially more numerous than those considered here. Nevertheless, the effect on the estimated LCB would never be greater than 2–4 kJ mol<sup>-1</sup>, since the population of species with larger energy gaps than the most stable ones would be negligible.

**Torsional barriers:** In the analysis in the previous section we have assumed implicitly that, under the experimental conditions, the system has enough internal energy to allow the alkyl chain of the benzene derivative to coil up. To confirm that this is indeed the case it would be necessary to estimate the barriers involved in the corresponding torsions. For the case of *n*-butylbenzene, the torsion barriers were estimated by increasing the value of  $\phi$  and  $\theta$  (defined in Figure 2) in 5° steps, starting from the completely extended **nBut1** conformer. For the corresponding potential-energy curves, see Figure 3.

To the best of our knowledge, these torsional barriers are not known experimentally. Nevertheless, our calculated barriers, 14 and 12 kJ mol<sup>-1</sup> respectively, are in very good

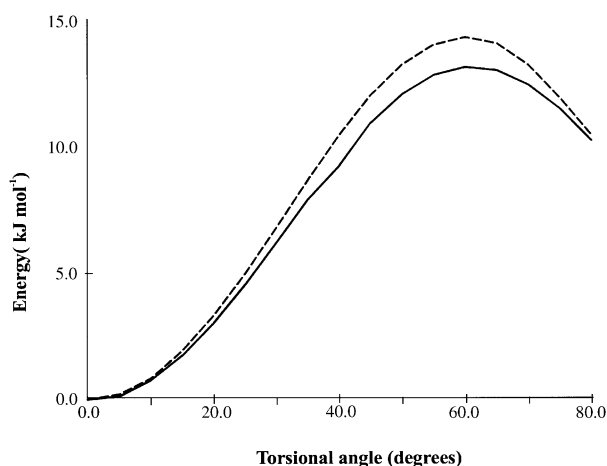


Figure 3. Potential-energy curve corresponding to the C2–C3 torsion ( $\phi$ ) (broken line) and C3–C4 torsion ( $\theta$ ) (solid line) in *n*-butylbenzene. Energy values are relative to the most stable conformer.

agreement with the experimental rotational barrier for ethane ( $12.00 \pm 0.04 \text{ kJ mol}^{-1}$ ).<sup>[53]</sup> Importantly, these values are much smaller than the interaction energy between  $B_{\text{ref}}\text{Li}^+$  and  $B =$  alkylbenzene when they approach to exchange  $\text{Li}^+$ . Therefore, in principle, the system should have enough internal energy to overcome these torsional barriers. In fact, the torsion displacements take place in the presence of approaching  $B_{\text{ref}}\text{Li}^+$ , that is, in the presence of a coulombic field. To estimate this electric field effect, we re-evaluated the corresponding torsional barriers in the presence of a point charge situated successively on the three axes and at two different distances from the molecule, namely 4.8 and 4.0 Å, respectively. The energies were calculated for the points along the potential-energy curves of Figure 3. The energy values for the minimum and the maximum of the potential-energy curve corresponding to the  $\phi$  torsion are given in Table 4. Although the total energies change significantly due to the presence of the field, the value of the torsional barrier remains practically unchanged, the differences from the zero-field situation being typically smaller than  $1 \text{ kJ mol}^{-1}$ . Hence, we can safely conclude that, under the normal experimental conditions, the system has enough internal energy to allow the coiling of the alkyl chain in order to enhance its interaction with the metal cation, giving rise to the “scorpion effect”.

## Conclusion

Our results show that for *n*-butylbenzene and *n*-heptylbenzene, the most stable complexes correspond to  $\pi$  complexes in which the alkyl chain coils up toward the aromatic ring to favor its interaction with the metal, by the so-called scorpion effect. Quite importantly, these coiled conformations are among the least stable in the neutral system, and many of them are not even minima of the potential-energy surface. The formation of these complexes leads to a significant enhancement of the  $\text{Li}^+$  binding energies (LBEs), which are found to be  $20\text{--}30 \text{ kJ mol}^{-1}$  higher than those estimated for “non-scorpion”  $\pi$  complexes, that is, in the absence of interaction between the metal and the alkyl chain. This enhancement is less significant for LCBs because the scorpion effect is entropically disfavored. There is very good agreement between the calculated LCBs and those measured by means of FT-ICR mass spectrometry, provided that the calculation of the former takes into account the statistical distribution of the different conformers present in the gas phase.

Alkali metal cations interact with organic species through mainly electrostatic forces, and nonpolar moieties may be weak ligands in this regard. Nevertheless the so-called cation– $\pi$  interaction, involving aromatic rings, has been shown to play an important role in biological systems. Gokel and co-workers<sup>[54]</sup> recently advocated the inclusion of the cation– $\pi$  interaction in the panoply of feeble forces to be taken into account in molecular recognition and supramolecular chemistry. In this regard, the scorpion effect, as a mechanism that enhances the cation– $\pi$  interactions of alkali metals with arenes, acquires a broader significance.

## Experimental Section

All compounds used for the FT-ICR measurements (the chemicals in Table 1, lithium benzoate, and 2-chloropropane) were of commercial origin (Aldrich, Fluka) and of the highest purity available. Gas-phase reactants were introduced in the vacuum system of the spectrometer without further purification, except degassing by several freeze–pump–thaw cycles. The electromagnet FT-ICR spectrometer at the University of Nice-Sophia Antipolis, using Bruker CMS 47 electronics, has been described elsewhere.<sup>[55]</sup>

Table 4. Effect of an external positive charge on the DFT-calculated energies ( $E$  [hartrees]) for the minimum and the maximum of the potential-energy curve corresponding to the  $\phi$  torsion of the alkyl chain of *n*-butylbenzene, and energy barriers ( $\Delta E$  [ $\text{kJ mol}^{-1}$ ]). Values in the presence or absence of a coulombic field created by a point charge have been calculated.

	No field		Field 1 <sup>[a]</sup>						Field 2 <sup>[b]</sup>					
	$E$	$\Delta E$	$x$ $E$	$\Delta E$	$y$ $E$	$\Delta E$	$z$ $E$	$\Delta E$	$x$ $E$	$\Delta E$	$y$ $E$	$\Delta E$	$z$ $E$	$\Delta E$
minimum	–389.50794		–389.50830		–389.51162		–389.52546		–389.50856		–389.51337		–389.53517	
maximum	–389.50247	14.4	–389.50271	14.7	–389.50603	14.7	–389.51980	14.9	–389.50304	14.5	–389.50783	14.5	–389.52962	14.6

[a] Field created by a positive point charge located 4.8 Å away from the molecule and along the three axes. [b] Field created by a positive point charge located 4.0 Å away from the molecule and along the three axes.



## Acknowledgement

This work has been partially supported by the DGI Project No. BQU2000–0245 and by the Picasso Project HF2000–0040. A generous allocation of computational time at the CCC of the Universidad Autónoma de Madrid is also gratefully acknowledged.

- [1] R. W. Taft, F. Anvia, J.-F. Gal, S. Walsh, M. Capon, M. C. Holmes, K. Hosn, G. Oloumi, R. Vasanwala, S. Yazdani, *Pure Appl. Chem.* **1990**, *62*, 17.
- [2] B. C. Guo, J. W. Purnell, A. W. Castleman Jr., *Chem. Phys. Lett.* **1990**, *168*, 155–160.
- [3] D. A. Dougherty, D. A. Stauffer, *Science* **1990**, *250*, 1558–1560.
- [4] R. A. Kumpf, D. A. Dougherty, *Science* **1993**, *261*, 1708–1710.
- [5] J. C. Ma, D. A. Dougherty, *Chem. Rev.* **1997**, *97*, 1303–1324.
- [6] J. B. Nicholas, B. P. Hay, D. A. Dixon, *J. Phys. Chem. A* **1999**, *103*, 1394–1400.
- [7] D. Feller, D. A. Dixon, J. B. Nicholas, *J. Phys. Chem. A* **2000**, *104*, 11414–11419.
- [8] V. Ryzhov, R. C. Dunbar, B. A. Cerda, C. Wesdemiotis, *J. Am. Soc. Mass Spectrom.* **2000**, *11*, 1037–1046.
- [9] R. D. Wieting, R. H. Staley, J. L. Beauchamp, *J. Am. Chem. Soc.* **1975**, *97*, 924–926.
- [10] R. H. Staley, J. L. Beauchamp, *J. Am. Chem. Soc.* **1975**, *97*, 5920–5921.
- [11] R. L. Woodin, J. L. Beauchamp, *J. Am. Chem. Soc.* **1978**, *100*, 501–508.
- [12] J. Sunner, K. Nishizawa, P. Kebarle, *J. Phys. Chem.* **1981**, *85*, 1814–1820.
- [13] R. G. Keese, A. W. Castleman, *J. Phys. Chem. Ref. Data* **1986**, *15*, 1011–1071.
- [14] P. Burk, I. A. Koppel, I. Koppel, R. Kurg, J.-F. Gal, P.-C. Maria, M. Herreros, R. Notario, J.-L. M. Abboud, F. Anvia, R. W. Taft, *J. Phys. Chem. A* **2000**, *104*, 2824–2833.
- [15] T. B. McMahon, G. Ohanessian, *Chem. Eur. J.* **2000**, *6*, 2931–2941.
- [16] M. T. Rodgers, P. B. Armentrout, *Mass. Spectrom. Rev.* **2000**, *19*, 215–247.
- [17] T. Fujii, *Mass Spectrom. Rev.* **2000**, *19*, 111–138.
- [18] Y. Apeloig, P. v. R. Schleyer, J. S. Binkley, J. A. Pople, W. L. Jorgensen, *Tetrahedron Lett.* **1976**, 3923–3926.
- [19] M. Alcamí, O. Mo, M. Yanez, *J. Phys. Chem.* **1989**, *93*, 3929–3936.
- [20] M. Alcamí, O. Mo, M. Yanez, F. Anvia, R. W. Taft, *J. Phys. Chem.* **1990**, *94*, 4796–4804.
- [21] M. Alcamí, O. Mo, J. J. G. De Paz, M. Yanez, *Theor. Chim. Acta* **1990**, *77*, 1–15.
- [22] J. Cioslowski, Q. Lin, *J. Am. Chem. Soc.* **1995**, *117*, 2553–2556.
- [23] S. Mecozzi, A. P. West Jr., D. A. Dougherty, *J. Am. Chem. Soc.* **1996**, *118*, 2307–2308.
- [24] B. Goldfuss, P. v. R. Schleyer, F. Hampel, *J. Am. Chem. Soc.* **1997**, *119*, 1072–1080.
- [25] Y. Tsang, F. M. Siu, N. L. Ma, C. W. Tsang, *Rapid Commun. Mass Spectrom.* **2002**, *16*, 229–237.
- [26] J.-F. Gal, P.-C. Maria, M. Decouzon, O. Mó, M. Yáñez, *Int. J. Mass Spectrom.* **2002**, *219*, 445–456.
- [27] S. Hoyau, K. Norrman, T. B. McMahon, G. Ohanessian, *J. Am. Chem. Soc.* **1999**, *121*, 8864–8875.
- [28] P. B. Armentrout, M. T. Rodgers, *J. Phys. Chem. A* **2000**, *104*, 2238–2247.
- [29] A. Tsarbopoulos, J. Allison, *J. Am. Chem. Soc.* **1985**, *107*, 5085–5093.
- [30] M. L. Larrivee, J. Allison, *J. Am. Chem. Soc.* **1990**, *112*, 7134–7140.
- [31] D. J. Hankinson, C. B. Miller, J. Allison, *J. Phys. Chem.* **1989**, *93*, 3624–3630.
- [32] T. Pruesse, J. Allison, H. Schwarz, *Int. J. Mass Spectrom. Ion Processes* **1991**, *107*, 553–557.
- [33] R. M. Stepnowski, J. Allison, *Organometallics* **1988**, *7*, 2097–2103.
- [34] C. B. Lebrilla, C. Schulze, H. Schwarz, *J. Am. Chem. Soc.* **1987**, *109*, 98–100.
- [35] M. C. Holthausen, G. Hornung, D. Schroeder, S. Sen, W. Koch, H. Schwarz, *Organometallics* **1997**, *16*, 3135–3147.
- [36] K. Eller, H. Schwarz, *Chem. Rev.* **1991**, *91*, 1121–1177.
- [37] T. Pruesse, C. B. Lebrilla, T. Drewello, H. Schwarz, *J. Am. Chem. Soc.* **1988**, *110*, 5986–5993.
- [38] H. Schwarz, *Acc. Chem. Res.* **1989**, *22*, 282–287.
- [39] J. L. M. Abboud, M. Yanez, J. Elguero, D. Liotard, M. Essefar, M. El Mouhtadi, R. W. Taft, *New J. Chem.* **1992**, *16*, 739–745.
- [40] O. Tapia, R. Cárdenas, Y. G. Smeyers, A. Hernández-Laguna, J. J. Ráñez, F. J. Ráñez, *Int. J. Quant. Chem.* **1990**, *115*, 1450–1454.
- [41] M. Herreros, J. F. Gal, P. C. Maria, M. Decouzon, *Eur. Mass Spectrom.* **1999**, *5*, 259–265.
- [42] L. Z. Chen, R. Flammang, A. Maquestiau, R. W. Taft, J. Catalán, P. Cabildo, R. M. Claramunt, J. Elguero, *J. Org. Chem.* **1991**, *56*, 179–182.
- [43] S. M. Free, J. W. Wilson, *J. Med. Chem.* **1964**, *7*, 395–399.
- [44] M. J. Frisch, G. W. Trucks, H. B. Schlegel, G. E. Scuseria, M. A. Robb, J. R. Cheeseman, V. G. Zakrzewski, J. J. A. Montgomery, R. E. Stratmann, J. C. Burant, S. Dapprich, J. M. Millam, A. D. Daniels, K. N. Kudin, M. C. Strain, O. Farkas, J. Tomasi, V. Barone, M. Cossi, R. Cammi, B. Mennucci, C. Pomelli, C. Adamo, S. Clifford, J. Ochterski, G. A. Petersson, P. Y. Ayala, Q. Cui, K. Morokuma, D. K. Malick, A. D. Rabuck, K. Raghavachari, J. B. Foresman, J. Cioslowski, J. V. Ortiz, B. B. Stefanov, G. Liu, A. Liashenko, P. Piskorz, I. Komaromi, R. Gomperts, R. L. Martin, D. J. Fox, T. Keith, M. A. Al-Laham, C. Y. Peng, A. Nanayakkara, C. Gonzalez, M. Challacombe, P. M. W. Gill, B. Johnson, W. Chen, M. W. Wong, J. L. Andres, C. Gonzalez, M. Head-Gordon, E. S. Replogle, J. A. Pople, Gaussian98, Version A3, Gaussian, Inc., Pittsburgh (PA), **1999**.
- [45] A. D. Becke, *Phys. Rev. A* **1988**, *38*, 3098–3100.
- [46] A. D. Becke, *J. Chem. Phys.* **1993**, *98*, 1372–1377.
- [47] C. Lee, W. Yang, R. G. Parr, *Phys. Rev. B* **1988**, *37*, 785–789.
- [48] A. Luna, M. Alcamí, O. Mo, M. Yanez, *Chem. Phys. Lett.* **2000**, *320*, 129–138.
- [49] S. J. Klippenstein, C.-N. Yang, *Int. J. Mass Spectrom.* **2000**, *201*, 253–267.
- [50] A. Hernández-Laguna, J.-L. M. Abboud, R. Notario, H. Homan, Y. G. Smeyers, *J. Am. Chem. Soc.* **1993**, *115*, 1450–1454.
- [51] E. D. Raczynska, M. Darowska, M. K. Cyrański, M. Makowski, T. Rudka, J.-F. Gal, P.-C. Maria, *J. Phys. Org. Chem.*, in press.
- [52] N. S. Zefirov, V. V. Samoshin, O. A. Sobbotin, T. G. Zemyanova, G. M. Akhmetova, *Zh. Org. Khim.* **1987**, *23*, 1320–1322.
- [53] E. Hirota, Y. Endo, S. Saito, *J. Mol. Spectrosc.* **1981**, *89*, 285–295.
- [54] G. W. Gokel, L. J. Barbour, R. Ferdani, J. Hu, *Acc. Chem. Res.* **2002**, *35*, 878–886.
- [55] P. Boisson, M. Decouzon, J.-F. Gal, P.-C. Maria, A. Pagliardini, *Analisis* **1995**, *23*, 441–447.
- [56] J.-F. Gal, P.-C. Maria, M. Decouzon, O. Mó, M. Yáñez, J.-L. M. Abboud, *J. Am. Chem. Soc.*, in press.

Received: February 20, 2003 [F4863]